Published in final edited form as:
*J Biogeogr*. 2010 November ; 37(11): 2111–2124. doi:10.1111/j.1365-2699.2010.02368.x.

# Phylogeographic patterns of genetic diversity in eastern Mediterranean water frogs have been determined by geological processes and climate change in the Late Cenozoic

**Çiğdem Akın**[1,2], **C. Can Bilgin**[1], **Peter Beerli**[3], **Rob Westaway**[4], **Torsten Ohst**[2], **Spartak N. Litvinchuk**[5], **Thomas Uzzell**[6], **Metin Bilgin**[7], **Hansjürg Hotz**[2,8], **Gaston-Denis Guex**[8], and **Jörg Plötner**[2]

[1]Biodiversity and Conservation Laboratory, Department of Biological Sciences, Middle East Technical University, 06531 Ankara, Turkey [2]Museum für Naturkunde, Leibniz-Institut für Evolutions- und Biodiversitätsforschung an der Humboldt-Universität zu Berlin, Invalidenstraβe 43, 10115 Berlin, Germany [3]Department of Scientific Computing, Florida State University, Tallahassee, FL 32306-4120, USA [4]Faculty of Mathematics, Computing and Technology, The Open University, Abbots Hill, Gateshead NE8 3DF, UK, and IRES, Newcastle University, Newcastle-upon-Tyne NE1 7RU, UK [5]Institute of Cytology, Russian Academy of Sciences, Tikhoretsky prospekt 4, 194064 St. Petersburg, Russia [6]Laboratory for Molecular Systematics and Ecology, Academy of Natural Sciences, 1900 B. F. Parkway, Philadelphia, PA 19103, USA [7]Edward R. Madigan Laboratory, Department of Cell and Developmental Biology, University of Illinois at Urbana Champaign, Urbana, IL 61801, USA [8]Institut für Evolutionsbiologie und Umweltwissenschaften, Universität Zürich-Irchel, Winterthurerstrasse 190, 8057 Zurich, Switzerland

## Abstract

**Aim—**Our aims were to assess the phylogeographic patterns of genetic diversity in eastern Mediterranean water frogs and to estimate divergence times using different geological scenarios. We related divergence times to past geological events and discuss the relevance of our data for the systematics of eastern Mediterranean water frogs.

**Location—**The eastern Mediterranean region.

**Methods—**Genetic diversity and divergence were calculated using sequences of two protein-coding mitochondrial (mt) genes: ND2 (1038 bp, 119 sequences) and ND3 (340 bp, 612 sequences). Divergence times were estimated in a Bayesian framework under four geological scenarios representing alternative possible geological histories for the eastern Mediterranean. We then compared the different scenarios using Bayes factors and additional geological data.

Correspondence: Çiğdem Akın, Middle East Technical University, Department of Biological Sciences, Biodiversity and Conservation Laboratory, 06531 Ankara, Turkey. Tel: +90 312 210 50 45; Fax: +90 312 210 79 76; acigdem@metu.edu.tr.

**Supporting Information**

Additional Supporting Information may be found in the online version of this article:

**Appendix S1** Map of the eastern Mediterranean region.

**Appendix S2** Origin and haplotype information of the water frogs investigated.

**Appendix S3** Median joining network of ND3 sequences of Western Palaearctic water frogs.

**Appendix S4** Arithmetic means and standard deviations of genetic distances calculated between the main mitochondrial haplogroups of Western Palaearctic water frogs.

Author contributions: J.P., C.B., G.-D.G. and H.H. initiated the project; Ç.A, T.O. and M.B. provided mtDNA sequences and collected the data; Ç.A., P.B. and J.P. analysed the data; Ç.A, C.B., H.H., G.-D.G., T.U. and S.N.L. collected tissue samples; Ç.A, C.B., T.U., P.B., R.W. and J.P. were involved in writing the manuscript.

**Results—**Extensive genetic diversity in mtDNA divides eastern Mediterranean water frogs into six main haplogroups (MHG). Three MHGs were identified on the Anatolian mainland; the most widespread MHG with the highest diversity is distributed from western Anatolia to the northern shore of the Caspian Sea, including the type locality of *Pelophylax ridibundus*. The other two Anatolian MHGs are restricted to south-eastern Turkey, occupying localities west and east of the Amanos mountain range. One of the remaining three MHGs is restricted to Cyprus; a second to the Levant; the third was found in the distribution area of European lake frogs (*P. ridibundus* group), including the Balkans.

**Main conclusions—**Based on geological evidence and estimates of genetic divergence we hypothesize that the water frogs of Cyprus have been isolated from the Anatolian mainland populations since the end of the Messinian salinity crisis (MSC), i.e. since *c*. 5.5-5.3 Ma, while our divergence time estimates indicate that the isolation of Crete from the mainland populations (Peloponnese, Anatolia) most likely pre-dates the MSC. The observed rates of divergence imply a time window of *c*. 1.6-1.1 million years for diversification of the largest Anatolian MHG; divergence between the two other Anatolian MHGs may have begun about 3.0 Ma, apparently as a result of uplift of the Amanos Mountains. Our mtDNA data suggest that the Anatolian water frogs and frogs from Cyprus represent several undescribed species.

### Keywords

Divergence time; eastern Mediterranean; genetic diversity; geology; molecular clock; mtDNA; *Pelophylax* (*Rana*); phylogeography; speciation; water frogs

## INTRODUCTION

With its diverse topography and climate, the eastern Mediterranean region has served as an important corridor for faunal and floral interchanges both north–south and east–west (e.g., Kosswig, 1955). It is an important area for studying the phylogeography and speciation in plants and animals. Much is known about the Miocene and Pliocene geological and climatic history of the eastern Mediterranean region, which offers the possibility of analysing the processes that have affected patterns of biodiversity in this region.

Beginning about 15 Ma, progressive isolation of the Mediterranean Sea from the Atlantic Ocean to the west and the Indian Ocean to the east produced dramatic changes in terrestrial environments of the Mediterranean region. At the start of this period, progressive uplift of the northern Arabian Platform closed the ‘Tethyan Seaway’ that linked the Mediterranean Sea to the Indian Ocean, creating a quite narrow north–south land bridge between the Gaziantep area of central-southern Turkey and the Aleppo area of north-west Syria (e.g., Steininger & Rögl, 1984; localities shown in Appendix S1 in the Supporting Information). The former southward drainage from eastern Anatolia into this seaway was thus divided (e.g., Demir *et al.*, 2008), so that the Ceyhan was the easternmost river system flowing into the Mediterranean and the Euphrates and other rivers farther east flowed into a vast wetland environment, known as the Mesopotamian Basin, that occupied north-eastern Syria, much of Iraq, and western and SW Iran (e.g., James & Wynd, 1965; Ponikarov *et al.*, 1967). Migration of animals between Eurasia and Africa would have been possible as soon as the land bridge at the western end of the Mesopotamian Basin developed.

The Mediterranean Sea remained connected to the Atlantic Ocean until the uplift of Spain and Morocco gradually closed a series of seaways around 6 Ma (e.g., Krijgsman *et al.*, 1999a, b). Because evaporation was no longer balanced by inflow from the Atlantic, the Mediterranean Basin became desiccated at this time (e.g., Hsü *et al.*, 1973), which is known as the ‘Messinian salinity crisis’ or MSC (the name ‘Messinian’ refers to the Messinian

stage, the latest stage of the Miocene epoch, which lasted from 7.2 to 5.3 Ma). The MSC can be subdivided into an evaporitic phase and a post-evaporitic phase or Lago-Mare phase (5.61-5.33 Ma). In the Lago-Mare phase the Mediterranean Basin was partially re-flooded. The resulting lacustrine environment is known as the Lago-Mare basin; this phase is characterized by a transition from hypersaline to hyposaline conditions (e.g., Bassetti *et al.*, 2004; Sampalmieri *et al.*, 2009). Subsequent headward erosion by rivers in the westernmost Mediterranean Basin led to the breaching of the Atlantic Ocean through the Strait of Gibraltar (e.g., Loget *et al.*, 2005; Garcia-Castellanos *et al.*, 2009), which rapidly restored the sea level to that of the global ocean; this event defines the start of the Pliocene epoch. The MSC thus created a range of environments, some hostile and others favourable to plants and animals. In this context, the Mediterranean islands may have acted as stepping stones in a hostile environment. It is widely assumed that salt water-sensitive animals such as amphibians were able to migrate from the mainlands to the islands and vice versa, especially during the Lago-Mare phase. Hence, the putative isolation time (ca. 5 Myr) of the two largest islands in the eastern Mediterranean, Cyprus and Crete, has been used to calibrate molecular clocks (e.g., Beerli *et al.*, 1996; Gantenbein & Keightley, 2004; Lymberakis *et al.*, 2007).

In addition to geological processes, climate oscillations during the Late Cenozoic help explain the genetic diversity of plant and animal lineages in the eastern Mediterranean region (e.g., Médail & Diadema, 2009). Climate cyclicity, caused by precession and obliquity variation of the Earth's rotation axis (characteristic periods ~20 kyr and ~40 kyr, respectively), and fluctuations in the eccentricity of the Earth's orbit (characteristic period ~100 kyr) have occurred throughout the geological record. During the Late Cenozoic, the ~40 kyr Milankovitch periodicity predominated until the late Early Pleistocene, being superseded circa 0.9 Ma by the onset of ~100 kyr periodicity, with more severe cold stages (e.g., Mudelsee & Schulz, 1997); this change is known as the 'Mid-Pleistocene Revolution' (MPR) in climate. The latter climate transition involved a complex sequence of changes in ocean circulation and ice-sheet dynamics, lasting from ~1.3 Ma to ~0.7 Ma (Sosdian & Rosenthal, 2009); the first cold stage comparable in magnitude to the subsequent Middle and Late Pleistocene glaciations occurred at ~0.9 Ma.

An additional geological factor that had a great impact on biodiversity in the eastern Mediterranean region is the systematic increase in topographic relief that developed during the Late Cenozoic. Long dismissed or regarded as inexplicable (e.g., Molnar & England, 1990; Hay *et al.*, 2002), this effect is now thought to be a consequence of long time-scale climate change through its effect on rates of surface processes such as erosion; erosional unloading of the Earth's continental crust has resulted in uplift (e.g., Westaway *et al.*, 2009a). Three different phases of Late Cenozoic vertical crustal motion induced by climate change have been recognized in the eastern Mediterranean and surrounding regions. The earliest of these phases began circa 3.1 Ma, at the start of climate deterioration following the Mid-Pliocene climatic optimum. The second phase, which began circa 2 Ma, corresponds to the Pleistocene deterioration in Northern Hemisphere climate. The clearest of these phases, first recognized decades ago (Kukla, 1975, 1977, 1978), followed the MPR.

Because they represent a phylogenetically diverse but small radiation with different levels of molecular and organismal differentiation (reviewed by Plötner, 2005), water frogs are an ideal group with which to study the effects of geological processes and past climatic changes on patterns of biodiversity and phylogeography (Beerli *et al.*, 1996; Plötner *et al.*, in press). Water frogs occupy almost all suitable freshwater habitats, but their skin physiology makes them highly susceptible to arid climate and to isolation effects caused by hostile environments such as sea water, salt pans or deserts. If the geological age of isolation barriers is known, genetic distances between water frog populations separated by such

barriers can be used to calibrate molecular clocks (Beerli *et al.*, 1996). The refilling of the Mediterranean Basin at the end of the MSC, circa 5.5-5.3 Ma, has been considered as an event that has isolated water frog populations of Crete and Cyprus from the mainlands (Peloponnese/Anatolia/the Levant) and from populations inhabiting Spain and North Africa. The marine flooding of the Mediterranean Basin at the end of the MSC took place rapidly (on a time-scale much shorter than the shortest period of Milankovitch forcing of sea-level fluctuation in the Atlantic Ocean; e.g., Garcia-Castellanos *et al.*, 2009). Isolation of water frog populations by this event can thus be regarded as synchronous throughout the Mediterranean region.

We present new mitochondrial (mt) DNA data, based on a large collection of water frogs from the eastern Mediterranean and neighbouring regions, that reveal a diversity of genetic lineages differentiated in allopatry. We interpret these as a result of marine inundation, local and regional uplift, and climate change. The correlation of geological events with genetic data provides new insights into the evolution of eastern Mediterranean water frogs, including the phylogenetic age of different species and lineages. Our divergence time estimates, based on different geological scenarios concerning putative isolation times of Crete and Cyprus from the mainland (Greece, Anatolia, and the Levant), shed new light on the phylogenetic age of water frog populations of the eastern Mediterranean region. Moreover, our data are of general relevance for future studies on phylogeography, speciation, and molecular evolution of species distributed in the eastern Mediterranean region.

## MATERIALS AND METHODS

### Taxon sampling

A total of 612 water frog samples from 179 localities in western Asia, the Middle East (especially Anatolia), and surrounding regions, including the Levant, Central Asia, and Europe, were analysed (Appendix S2).

### DNA extraction, PCR, and sequencing

For most Anatolian samples, DNA was extracted from clipped toes. Homogenized tissue was digested in an extraction buffer, consisting of 3 M urea, 20 mM EDTA, 1% N-lauryl-sarcosine-Na-salt, 50 mM Tris-HCl pH 8.0, 125 mM $Na_2SO_4$, and 1% PVP, supplemented with 20 μg/ml proteinase K. After digestion, proteins were removed by phenol/chloroform/isoamyl alcohol (25:24:1) extraction. The aqueous phase containing DNA was air-dried with isopropanol at room temperature. DNA was pelleted, washed once with 70% ethanol before allowed to air-dry. Finally, DNA was eluted in TE buffer (pH 8.0) and stored at −20 °C. Tissue samples (muscle, liver) from ethanol-preserved material were soaked in three changes of distilled water over a 48 hr period. DNA was isolated from these samples with a QIAmp tissue kit (Qiagen GmbH, Hilden, Germany).

The ND2 gene sequence (1038 bp) was amplified with the primers ND2L1 (5’-AAGCTTTTGGGCCCATACCCC-3’), ND2H1 (5’-GGGGCGATTTTTTGTCAGGTTG-3’), ND2L2 (5’-GGACTCGCCCCYCTACACTTCTG-3’), ND2H2 (5’-CTCCGCTTAAGGCTTTGAAGGC-3’), ND2L3 (5’-RTCATAACRGCTTCTATATTYTT-3’), and ND2H3 (5’-TRTTGTTTTACYAGTTCMAGGG-3’); the ND3 gene (340 bp) with the forward primer ND3L (5’-TTGAGCCGAAATCAACTGTC-3’) and the reverse primer ND3H (5’-AGTACACGTGACTTCCAATC-3’) (Meyer, 1993; modified).

ND2 amplification involved an initial incubation at 94 °C for 1 min, followed by 35 cycles at 94 °C for 30 s, 62 °C for 20 s, and 72 °C for 60 s, and a final 7 min extension at 72 °C (Plötner *et al.*, 2008). Each ND3 amplification involved an initial incubation at 94 °C for 1 min, followed by 35 cycles at 94 °C for 30 s, 50 °C for 20 s, and 72 °C for 60 s, and a final 7 min extension at 72 °C. Polymerase chain reaction (PCR) products were purified with QIAquick PCR purification kits (Qiagen) or Gene Mark gel extraction kits (Hopegen Biotechnology, Dali City, Taiwan).

Sequencing reactions were performed with a Big Dye Ready Reaction Terminator Cycle Sequencing Kit (Applied Biosystems, Foster City, CA, USA) or a DYEnamic ET Terminator Cycle Sequencing Kit (Amersham, Piscataway, NJ, USA). Electrophoresis and detection of fluorescent dye-labelled nucleotide fragments were carried out with automatic DNA sequencers (ABI Prism 377 and ABI Prism 310 Genetic Analyzer, Applied Biosystems). The sequenced genes correspond to positions 6546–7583 (ND2) and 12089–12428 (ND3) in the genome of *Pelophylax nigromaculatus* (AB043889, Sumida *et al.*, 2001). Sequences representing new mitochondrial haplotypes were deposited in the EMBL Nucleotide Sequence Database under accession numbers listed in Appendix S2.

## Data analysis

Sequences were aligned using the CLUSTAL W algorithm in MEGA 4.1 (Tamura *et al.*, 2007). Nucleotide composition and number of variable sites were analysed with the same program. Haplotype frequency and diversity ($h$), and nucleotide diversity ($\pi$) (Nei, 1987) were calculated via Arlequin 3.01 (Excoffier *et al.*, 2005).

Models of sequence evolution and corresponding parameters were estimated for frogs of the *P. ridibundus* group (including *P. bedriagae*) with MODELTEST Server 1.0 (http://darwin.uvigo.es/software/modeltest_server.html;Posada, 2006) running MODELTEST 3.8 (Posada & Crandall, 1998). We used hierarchical likelihood ratio tests (hLRTs) and the Bayesian information criterion (BIC) to select a model of sequence evolution from a pool of candidate models. The best-fit model of sequence evolution for the concatenated ND2 and ND3 sequences was the Tamura–Nei (TrN) model (Tamura & Nei, 1993) with a gamma distribution (G) for site mutation rate (shape parameter = 0.2). All distance calculations were done with MEGA 4.1 (Beta 2).

A haplotype phylogeny based on the 83 unique concatenated ND2 and ND3 sequences (Appendix S2) was estimated using Bayesian inference as implemented in MRBAYES 3.1.2 (Ronquist & Huelsenbeck, 2003; Huelsenbeck & Ronquist, 2005). For the analysis, the general time reversible model, with corrections for invariant characters and gamma distributed rate heterogeneity (GTR+I+G) was applied as recommended by Huelsenbeck & Rannala (2004). Mutation model parameters were estimated from the data set. Posterior probabilities of phylogenetic trees were calculated by employing a $10^7$-iteration Metropolis-coupled Markov chain Monte Carlo (four chains, chain temperature parameter = 0.2). Trees were sampled every 1000 generations; the first 1000 recorded trees were discarded; 9000 recorded trees were examined. The autocorrelation of samples in the Markov chain was explored with internal program statistics. Additionally, a median-joining network (Bandelt *et al.*, 1999) was constructed with only ND3 sequences ($N$=116, Appendix S3), using the program NETWORK 4.5.0.1 (available at http://www.fluxus-engineering.com/sharenet.htm) with epsilon=0 to exclude less parsimonious pathways from the graph. For outgroup comparisons, mtDNA sequences from *P. cretensis*, *P. epeiroticus*, *P. bergeri*, *P. lessonae*, *P. perezi*, *P. saharicus*, *P. shqipericus*, and *P. nigromaculatus* were used (Appendix S2).

Tree topologies and TrN+G distances based on concatenated ND2 and ND3 sequences were used to define main haplogroups (MHGs). MHGs, subgroups, and corresponding haplotypes

were denoted as follows: MHG1 (*ridibundus*, Europe), R1.RE1-R18.RE11; MHG2 (*bedriagae*, the Levant), B1.BN1-B6.BN4; MGH3 (Cyprus), CP1.CY1-CP2.CY1; MHG4 (Cilician West), CL1.CI1-CL4.CL1; MHG5 (Cilician East), CL5.CI10-CL8.CI9; MHG6 (cf. *bedriagae*, Anatolia), A1.AN12-A40.AN55; MHG7 (Central Asia 1), C1.CA5-C3.CA13; MHG8 (Central Asia 2), C4.CA14-C5.CA14; and MHG9 (Middle East), M1.ME1. MHG6 was itself subdivided, MHG6a (cf. *caralitanus*), A1.AN12-A5.AN1; MHG6b (cf. *cerigensis*), A6.AN21-A11.AN25; MHG6c (cf. *bedriagae* sensu stricto), A12.AN54-A35.AN43; and MHG6d (Euphrates), A36.AN43-A40.AN55 (Fig. 1, Appendix S2).

Divergence times were estimated on the basis of the 83 unique concatenated ND2 + ND3 sequences with three different methods: (1) a Bayesian approach using the program BEAST (Drummond & Rambaut, 2007); (2) a simplified linear regression model, dividing pairwise TrN+G distances by constant evolutionary rates (1.6 and 1.7% per Myr) calculated on the basis of two putative divergence time values (5.3 and 5.5 Myr) for the isolation between Cyprus and Anatolian water frog populations as a calibration point (the mean TrN+G value between Cyprus and Anatolian frogs was 0.0899); and (3) direct estimation on a neighbour-joining (NJ) tree, calculated on the basis of TrN+G distances with the assumption of heterogeneous substitution patterns among lineages, as implemented in MEGA 4.1 (Tamura *et al.*, 2007).

Geological events have been used in many biogeographical studies, but often there is considerable uncertainty about their timing. A date of isolation commonly used is the end of the MSC circa 5.3 Ma; this has often been considered a minimum isolation time for both Crete and Cyprus. Recent molecular data, however (e.g., Plötner *et al.*, 2001, in press; Kasapidis *et al.*, 2005; Parmakelis *et al.*, 2005, 2006), in concert with geological data (e.g., Frydas & Keupp, 1996, 2001; Hardie & Lowenstein, 2004; Cosentino *et al.*, 2007), suggest an earlier isolation of Crete, perhaps as early as 9 Ma. Therefore, the confidence intervals for the minimum isolation time of Cyprus are thought to be narrow whereas the confidence intervals for the isolation time of Crete are unknown.

In the Bayesian framework of BEAST, the times of internal nodes of the phylogeny can be associated with prior distributions that reflect prior knowledge about the time of speciation events associated with that node. We explored the power of our data to distinguish between four geological scenarios, representing alternative possible geological histories of the eastern Mediterranean region. For each of these alternatives, we specified as prior distributions two normal distributions: using putative times of the isolation of Cyprus (5.3 Ma) and of Crete (5.3 or 9.0 Ma) from the mainlands as the means and two different standard deviation values: narrow (n) values of ±0.3 Myr and wide (w) values correspond to half of the isolation time (±4.5 and ±2.65 Myr for 5.3 and 9.0 Ma, respectively). The narrow standard deviation for the isolation of Cyprus is based on geological evidence and the palaeogeography of this region during the MSC. The values for Crete, in contrast, are informed guesses, taking account of the greater uncertainty in the palaeogeography of Crete during the Late Miocene (discussed by Plötner *et al.*, in press).

BEAST was run for each scenario using input files constructed from the MrBayes input files with BEAUti, using a relaxed clock model that allows for differences between evolutionary rates among lineages; the rates were drawn from a lognormal prior distribution assuming that rates are not correlated. The trees were formed using a Yule prior, with the constraint that the lineages leading to individuals from Cyprus and from Crete were defined by the divergence time prior. Divergence times of clades were recorded without assuming that these clades always represent monophyletic groups, except for the split of the Western Palaearctic water frogs from their Eastern Palaearctic relatives, which was forced to form

two monophyletic groups. Mutation rate was estimated using the TN93 model with site rate variation.

Each scenario was run five times with a burn-in of $10^6$ iterations and $10^7$ sampled iterations; subsequently the five replicates were combined in TRACER (http://tree.bio.ed.ac.uk/software/tracer/) and analysed; marginal likelihood estimates were then used to calculate Bayes factors (Kass & Raftery, 1995). Bayes factors (BF) are a Bayesian equivalent of likelihood ratio tests. They do not require that the models be nested and provide a direct way to compare models without an *ad hoc* hierarchical analysis system, as used, for example, by nested clade phylogeographic analysis (NCPA; Templeton, 2004). BFs are, therefore, a good tool for comparisons of divergence models.

The program BEAST was also used to test whether the evolutionary rates in the phylogeny obey a strict or a relaxed molecular clock. The runtime parameters were identical to those described for the divergence model analysis, except that no constraints for divergence were used and the evolutionary rate model was set to either strict clock or a variable clock-model drawing evolutionary rates from a lognormal distribution.

## RESULTS

### Genetic diversity

The analysis utilized 119 ND2 and 612 ND3 sequences from frogs of the *P. ridibundus* group, including individuals from Anatolia, Cyprus, the Middle East, Central Asia, the Levant (*P. bedriagae*), and Central Europe (*P. ridibundus sensu stricto*; Appendix S2). The ND2 sequences contained 250 (24.1%) variable sites of which 222 (21.4%) are parsimony-informative. These ND2 sequences define 80 haplotypes with $h$=0.99±0.003 and $\pi$=4.37±2.10%. The ND3 sequences contained 100 variable sites (29.4%), of which 71 (20.9%) are parsimony-informative. They define 116 haplotypes; the haplotype diversity was $h$=0.96±0.004 and the nucleotide diversity was $\pi$=3.95±1.97%. The concatenated sequences (ND2+ND3; $N$=119) define 83 unique haplotypes (Fig. 2, Appendix S2); the ND2 sequence for both members of three pairs of the concatenated haplotypes was the same, although the two ND3 sequences of each pair differed.

### Phylogenetic analysis, genetic differentiation and geographical distribution of haplogroups

The topologies of the Bayesian tree calculated on the basis of the ND2 and ND3 genes (Fig. 2) and the median-joining network based only on ND3 sequences (Appendix S3), together with the geographic distribution patterns of haplotypes (Fig. 1) and pairwise TrN+G distances (Appendix S4), reveal 9 distinct MHGs, each supported by posterior probabilities of 1.0 in the Bayesian tree (Fig. 2). Mean TrN+G distances (G=0.2) between these MHGs ranged from 0.035 (MHG6-MHG7) to 0.124 (MHG1-MHG3); mean distance values within MHGs were ≤0.018.

MHG1 is characteristic of European *P. ridibundus*; it is widespread throughout Europe from France to central Russia. The highest haplotype diversity of MHG1 was observed in Greek populations, where 15 of the 18 haplotypes occur. Haplotypes R4.RE11-R18.RE11 are characteristic of Balkan lake frogs; R1.RE1-R3.RE1 are the most common haplotypes of Central European *P. ridibundus*.

MHG2 is characteristic of *P. bedriagae*; it was detected in Jordan, western Syria, and the Nile delta (Egypt). Divergence within this MHG is relatively high as indicated by a $\pi$-value of 1.2±0.73. MHG3 is restricted to Cyprus. MHG4 (Cilician West) and MHG5 (Cilician East) are sister groups (Fig. 1 and Fig. 2); haplotypes of MHG4 occur primarily in the

Cilician plain of southern Turkey, but also, although less frequently, east of the Amanos Mountains, together with haplotypes from MHG5. Haplotypes of MHG5 are distributed east of the Amanos Mountains in the Hatay, Kilis, Gaziantep, and especially Kahramanmaraş provinces of central-southern Turkey (Appendix S1).

MHG6 (cf. *bedriagae*, Anatolia) has the highest haplotype diversity ($h$=0.92±0.01) and nucleotide diversity ($\pi$=1.96%±0.01). It can be divided into four subgroups (a–d); mean distance values between these subgroups were 0.018–0.026. MHG6a (cf. *caralitanus*) is distributed mainly in southwestern Turkey (the Anatolian Lake District, the region around Beyşehir Lake, Konya, the type locality of *Pelophylax* cf. *caralitanus*). Haplotypes of this group were also found in northern Cyprus (A1.AN12) and on the Aegean island Ikaria (A3.AN19). MHG6b (cf. *cerigensis*) is restricted west of Antalya on the Mediterranean coast of southwestern Turkey; it also occurs on both Rhodos and Karpathos. MHG6c (cf. *bedriagae sensu stricto*) is the largest subgroup within MHG6; it is distributed from western Turkey to central Russia; it overlaps with MHG1 (*ridibundus*, Europe), for example, in Thrace, Russia, and the Caucasus (Fig. 1). Haplotypes of MHG6c were also found on the Aegean islands Samos, Lesvos, and Chios and at the restricted type locality of *P. ridibundus* (Atyrau, the northern shore of the Caspian Sea, in Kazakhstan). MHG6d (Euphrates) is distributed within the catchments of the rivers Euphrates and Tigris; it was found in eastern Anatolia where it coexists with haplotypes of MHG6c, in western Iran, and in north-eastern Syria.

MHG7 (Central Asia 1) was found south and east of the Caspian Sea, in Iran, Turkmenistan, and Uzbekistan; MHG8 (Central Asia 2) has been recorded in Kyrgyzstan and neighbouring parts of Kazakhstan, in the extreme east of our study area. MHG9 (Middle East) was found in Pasagard (southwest Iran).

## Estimation of divergence times

The global divergence time analysis with BEAST and the two other procedures (Table 1) reveal similar patterns, except that the methods based on pairwise comparisons (regression model) and on the NJ tree are less sophisticated and the corresponding ranges are probably too small. The BEAST analysis revealed only small statistical differences between the four geological scenarios; most credibility intervals of the time of divergence for particular clades overlap (Fig. 3). Crete appears to have become isolated before Cyprus but the posterior distributions of the divergence times overlap considerably. The scenario with strongly peaked prior distributions for the isolation of Crete and Cyprus achieved the highest marginal log likelihood (CRETE9n: −10,511.035±0.164), but the other scenarios report very similar values: CRETE9w has −10,511.474±0.177, CRETE5w has −10,511.623, and CRETE5n has −10,514.081. The largest difference among scenarios is 3.046 log likelihood units; using Kass & Raftery's (1995) guidelines, this difference suggests that the scenarios CRETE5n and CRETE9n are different. The other scenarios, however, are only 0.588 and 0.439 log likelihoods units apart from CRETE9n, suggesting that they cannot be rejected. Selecting among the four scenarios, using Kass & Raftery's (1995) approach, results in probabilities of 0.445, 0.287, 0.247, and 0.021 for CRETE9n, CRETE9w, CRETE5w, and CRETE5n, respectively. Thus, although the CRETE9n scenario (involving isolation of Crete circa 9 Ma and Cyprus circa 5.3 Ma) is the most probable scenario considered, other possible scenarios (e.g., isolation of Crete earlier than Cyprus, but not circa 9 Ma) cannot be ruled out.

The separation of the western Mediterranean species pair *P. saharicus* (North Africa) and *P. perezi* (Iberian Peninsula) is confirmed to have occurred before 5.3 Ma in all the analyses. BEAST also calculates a posterior estimate of the average expected mutation rate. The average mutation rate estimate for the best scenario was 0.00943 mutations per site per Myr

with a coefficient of variation of 1.112 indicating a standard deviation of 0.0105. A standard deviation of the magnitude of the mean suggests considerable mutation rate heterogeneity among lineages in the phylogeny. A comparison using BFs of the strict clock model versus the relaxed clock model with independent evolutionary rates and no divergence time constraints shows considerable support for the non-clock model. The marginal likelihoods were −10,546.547 and −10,510.856 for the clock and non-clock model, respectively. This results in strong support for the non-clock model with a ln BF of −35.69.

## DISCUSSION

### Implications for the development of the eastern Mediterranean region

The MSC can be expected to have had a great impact on biodiversity. Although this event is now well documented (e.g., Clauzon *et al.*, 1996; Krijgsman *et al.*, 1999a,b; Meijer & Krijgsman, 2005; Orszag-Sperber, 2006; Rouchy & Caruso, 2006; Roveri & Manzi, 2006), many details of chronology, depositional settings, hydrological mechanisms, and geochemical processes remain open to debate. The assumption, already mentioned, that Cyprus was not isolated from Anatolia during the Lago-Mare phase of the MSC but became isolated immediately thereafter, underpins our genetic analysis of eastern Mediterranean water frogs. Our divergence time estimates (Table 1) indicate that other lineages probably also became isolated from each other during the MSC or immediately thereafter.

The divergence times obtained from our relaxed clock model are statistically insufficient to choose among different isolation scenarios for Crete and Cyprus (Fig. 3). The results of phylogenetic analysis (Fig. 2) indicate, however, that Cretan water frogs diverged from the mainland populations before Cypriot water frogs did, suggesting that the isolation time of Cretan populations pre-dates the MSC. This deduction is consistent with geological evidence regarding the Late Miocene palaeogeography of the eastern Mediterranean region. During the evaporitic phase of the MSC, Cyprus was largely surrounded by playas (or salt pans) (e.g., Robertson, 1998); during the subsequent Lago-Mare phase, waters of the palaeo-lake covered these areas. Sediments of the Lago-Mare facies are found both offshore of Cyprus in boreholes and onshore in low-lying parts of the island; the latter deposits reflect subsequent uplift of the island, the water surface during the Lago-Mare phase having been far below modern sea-level. The Kyrenia (Beşparmak) mountain range of northern Cyprus is structurally connected to the Misis mountain range east of Adana in southern Turkey by the Misis-Kyrenia Fault Zone (MKFZ, Appendix S1), which forms part of the boundary between the Turkish and African plates. This fault zone became active around the start of the MSC (e.g., Robertson *et al.*, 2004;Westaway *et al.*, 2008) and forms a significant linear ridge, both onshore in Cyprus and offshore to the northeast, that is thought to have protruded above the level of evaporite deposition during the MSC. It probably also remained above the water level during the subsequent Lago-Mare phase, enabling migration of terrestrial animals between Anatolia and Cyprus until the restoration of marine conditions at ~5.3 Ma.

In contrast, Crete was surrounded by Messinian evaporite depocentres, parts of the island being low enough at the time (before subsequent uplift took place) to be covered by the evaporite. Cosentino *et al.* (2007) have shown that much, although not all, of Crete was subsequently inundated during the Lago-Mare phase. There is no evidence, however, of any adjoining geological structure, analogous to the MKFZ for Cyprus, that could have permitted migration of salt water-sensitive animals to or from Crete during the evaporitic phase or the Lago-Mare phase of the MSC; Crete was evidently an island, surrounded in all directions by tens or hundreds of kilometres of open salt water during the first of these phases and fresh or brackish water during the second; this is indicated, for example, by biostratigraphic evidence of continuous sedimentation across the Miocene/Pliocene boundary within the Maleme basin of Crete (Frydas & Keupp, 1996, 2001). Many local

animal and plant populations evidently became isolated before the MSC and survived its evaporitic phase, presumably in what are now the highest parts of the island, which were well above the contemporaneous playa level. It is thus hypothesized that Crete became separated from the mainland areas both to its west (the Peloponnesos) and to its east (Anatolia) by marine straits around 10-9 Ma (Dermitzakis & Papanikolaou, 1981; Welter-Schultes & Williams, 1999).

The Bayes factor comparison of the different geological scenarios is an important addition to the toolset for comparing genetic divergence pattern with geological patterns. Our findings make clear that a single locus, mtDNA, although highly informative for phylogeny of water frogs and sufficient to reveal the order of the divergence events, fails to give an unambiguous ranking of the alternative geological scenarios. Model ranking suggests that the scenario traditionally used in biogeographic studies of this region (CRETE5n) should be treated with caution because the scenarios CRETE9w and CRETE9n, suggesting that Crete was isolated before Cyprus, have a higher probability and are compatible with the available geological evidence (e.g., Frydas & Keupp, 1996, 2001). The scenario CRETE5w, however, which allows separation of Crete and Cyprus at the same time, but allows for more uncertainty for the separation time of Crete, cannot be distinguished from the scenarios that move the mean of the separation of Crete to an earlier date. This discrepancy suggests that, from a biological viewpoint, more evidence is needed to date the isolation of Crete precisely.

Estimating the time of geological events by molecular data is often error prone; different data sets may lead to controversial conclusions because of different evolutionary rates of single markers (e.g., Maca-Meyer *et al.*, 2003; Carranza *et al.*, 2006; Paulo *et al.*, 2008), gene flow between populations, bottleneck effects, and selection. Because the isolation time for Crete is not as precisely known as that for Cyprus, our estimates of divergence time for eastern Mediterranean water frog populations, although based on only a single DNA marker, are an improvement over an analysis based on protein electrophoretic data (Beerli *et al.*, 1996), which assumed a minimal separation time of Crete at 5 Ma.

### Historical phylogeography of Anatolian water frogs

The current mtDNA divergence among Anatolian water frogs appears to be the result of gradual genetic divergence in allopatry, closely associated with the geodynamic evolution of the Mediterranean since the Middle Miocene (i.e., since circa 11 Ma). Dispersal between populations has been prevented by the development of localized mountain ranges, waterless plateaux, and salt water barriers that have originated as a result of plate motions, regional uplift and subsidence, and environmental changes such as the MSC.

Our divergence time estimates indicate that Anatolian lineages diverged between circa 5 and 1 Ma (Table 1). The Cilician clades MHG4 and MHG5 may have split from the remaining Anatolian populations (MHG6) first, as indicated by divergence time values of 5.3-2.9 Ma (mean value calculated with BEAST: circa 4.5 Ma). This split was probably caused by uplift of the central Taurus Mountains during the Late Miocene and Pliocene (Jaffey & Robertson, 2005), although the timing of this uplift is not well constrained. In accordance with divergence time estimates of approximately 4.4-1.6 Ma (mean value calculated with BEAST circa 3.0 Ma), the separation of the Cilician clades from each other was probably caused by the uplift of the Amanos Mountains, which began ~3.7 or ~3.6 Ma as a result of a change in the pattern of plate motions in this region (Seyrek *et al.*, 2008a;Westaway *et al.*, 2008).

Circa 1.6-1.1 Ma the remaining Anatolian clade (MHG6) diverged into its 4 subgroups (a–d): cf. *caralitanus*, cf. *cerigensis*, cf. *bedriagae sensu stricto*, and ‘Euphrates’, with mean divergence values (TrN+G) of 1.8–2.6% (Table 1, Appendix S4). This was a time of

significant global cooling (e.g., Head & Gibbard, 2005;Ehlers & Gibbard, 2007;Sosdian & Rosenthal, 2009). Resulting from more rapid erosion consistent with the climate change around this time, increased rates of uplift occurred in some regions, for instance north of the Black Sea (e.g., Bridgland & Westaway, 2007), on the northern Arabian Platform in south-eastern Turkey and adjacent parts of Syria (Demir *et al.*, 2007,2008;Westaway *et al.*, 2009b), and in the eastern Taurus Mountains (Seyrek *et al.*, 2008b). These processes may have reduced distributional ranges and enhanced the isolation of different lineages.

### Implications for water frog systematics

Based on morphology alone, only a single water frog species, the lake frog *Pelophylax ridibundus* (Pallas, 1771), was reported from Turkey until the early 1990s (Bodenheimer, 1944; Başoğlu & Özeti, 1973; Andren & Nilson, 1976). Despite their great similarity in morphology (Jdeidi, 2000; J. Plötner unpublished data), Anatolian water frogs show considerable mtDNA divergence with TrN+G values >0.05 between MHGs 4, 5 and 6. Such values are characteristic of interspecific divergence in Western Palaearctic water frogs (J. Plötner, unpublished data), while the small genetic divergence values (0.018–0.026, Table 1) observed among the four subgroups (a–d) of the huge Anatolian MHG6 indicate conspecificity. The overlapping and intermixed distribution of MHG6 haplotypes across southern Anatolia suggests that there has been considerable mixing of distinct genetic stocks in this region (Akın *et al.*, 2010).

In contrast to bioacoustic data (e.g., Schneider & Sinsch, 1999), molecular data including mtDNA strongly suggest that Anatolian water frogs (MHG4, 5, and 6) and frogs from Cyprus (MHG3) are not conspecific with either Central European *P. ridibundus* (MHG1) (Beerli *et al.*, 1996; Plötner & Ohst, 2001) or *P. bedriagae* from the Levant (MHG2) (Plötner *et al.*, 2001, 2007, 2009, in press). The genetic distinctness of MHG3, which is also supported by nuclear DNA sequences (J. Plötner & C. Akın, unpublished data), warrants species status for Cypriot frogs (Plötner *et al.*, in prep.). To clarify the systematic status of the Anatolian water frogs, more investigations are needed, especially genomic and biogeographic analyses.

## Supplementary Material

Refer to Web version on PubMed Central for supplementary material.

## Acknowledgments

We thank Thomas Brachert (Leipzig), Wolfgang Kiesling (Berlin), and two anonymous reviewers for suggestions and advice. Grateful thanks are due to Robert Schreiber (Berlin) for technical assistance. For providing water frog samples we thank Wolfgang Böhme (Bonn), Daniel Frynta (Prague), Rainer Günther (Berlin), Petr Kotlik (Libechov), Peter Mikuliček (Prague), Dirk Schmeller (Saint Girons), and Mathias Stöck (Lausanne). We are grateful to the following people for assistance in the field: Onur and Selçuk Baloğlu, Banu Kaya, Senem Tuğ, Didem and Yakup Cakaroğulları, İbrahim Sözer, Mehmet Akın, Hüseyin Ambarlı, Damla Beton, Ayşe Turak, Ahmet and Bülent Akman, Yasemin Deveci, Ferhat Batur, Kurtuluş Olgun, Yüksel Güneş, Deniz Mengüllüoğlu, Soner Oruç, Tümay Becerancı, Sinan Fındık. Ayşe Turak helped prepare the maps. This research was supported by the Deutsche Forschungsgemeinschaft (grants PL 213/3-1, 3-2, 3-3) and the Swiss National Fund (grants 31-37579.93, 31-59144.99, 31-103903/1 and 31-64004.00). Çiğdem Akın and Can Bilgin were supported by METU Research Fund (BAP-08-11-DPT-2002K120510). Peter Beerli was partly supported by the joint NSF/NIGMS Mathematical Biology programme under NIH grant R01 GM 078985 and NSF grant DEB 0822626. Spartak N. Litvinchuk was partly supported by a DAAD grant under A/03/06782, a Presidium of RAS Program in Molecular and Cellular Biology, and RFBR grants under 08-04-01184, 09-04-10098, and 09-04-90475.

## REFERENCES

Akın Ç, Bilgin M, Bilgin CC. Discordance between ventral colour and mtDNA haplotype in the water frog *Rana* (*ridibunda*) *caralitana*, 1988 Arıkan. Amphibia-Reptilia. 2010; 31:9–20.

Andren C, Nilson G. Observations on the herpetofauna of Turkey in 1968 – 1973. British Journal of Herpetology, London. 1976; 5:575–584.

Bandelt H-J, Forster P, Röhl A. Median-joining networks for inferring intraspecific phylogenies. Molecular Biology and Evolution. 1999; 16:37–48. [PubMed: 10331250]

Bassetti MA, Manzi V, Lugli S, Roveri M, Longinelli A, Lucchi FR, Barbieri M. Paleoenvironmental significance of Messinian post-evaporitic lacustrine carbonates in the northern Apennines, Italy. Sedimentary Geology. 2004; 172:1–18.

Başoğlu, UM.; Özeti, N. Türkiye Amfibileri. Bornova, İzmir (in Turkish): 1973. p. 95-100.Ege Üniversitesi Fen Fakültesi Kitapları Serisi, No. 50

Beerli P, Hotz H, Uzzell T. Geological dated sea barriers calibrate a protein clock for Aegean water frogs. Evolution. 1996; 50:1676–1687.

Bodenheimer FS. Introduction into the knowledge of the Amphibia and Reptilia of Turkey. Istanbul Üniversitesi Fen Fakültesi Mecmuası. 1944; 9:12–13.

Bridgland DR, Westaway R. Preservation patterns of Late Cenozoic fluvial deposits and their implications: results from IGCP 449. Quaternary International. 2007; 189:5–38.

Carranza S, Arnold EN, Pleguezuelos JM. Phylogeny, biogeography, and evolution of two Mediterranean snakes, *Malpolon monspessulanus and Hemorrhois hippocrepis* (Squamata, Colubridae), using mtDNA sequences. Molecular Phylogenetics and Evolution. 2006; 40:532–546. [PubMed: 16679033]

Clauzon G, Suc J-P, Gautier F, Berger A, Loutre M-F. Alternate interpretation of the Messinian salinity crisis: Controversy resolved? Geology. 1996; 24:363–366.

Cosentino D, Gliozzi E, Pipponzi G. The late Messinian Lago-Mare episode in the Mediterranean Basin: Preliminary report on the occurrence of Paratethyan ostracod fauna from central Crete (Greece). Geobios. 2007; 40:339–349.

Demir T, Westaway R, Bridgland D, Pringle M, Yurtmen S, Beck A, Rowbotham G. Ar-Ar dating of Late Cenozoic basaltic volcanism in northern Syria: implications for the history of incision by the River Euphrates and uplift of the northern Arabian platform. Tectonics. 2007; 26 doi: 10.1029/2006TC001959.

Demir T, Seyrek A, Westaway R, Bridgland D, Beck A. Late Cenozoic surface uplift revealed by incision by the River Euphrates at Birecik, southeast Turkey. Quaternary International. 2008; 186:132–163.

Dermitzakis DM, Papanikolaou DJ. Paleogeography and geodynamics of the Aegean region during the Neogene. Annales Géologiques des Pays Helleniques. 1981; 30:245–289.

Drummond AJ, Rambaut A. BEAST: Bayesian evolutionary analysis by sampling trees. BMC Evolutionary Biology. 2007; 7:214. doi:10.1186/1471-2148-7-214. [PubMed: 17996036]

Ehlers J, Gibbard PL. The extent and chronology of Cenozoic global glaciation. Quaternary International. 2007; 164–165:6–20.

Excoffier L, Laval G, Schneider S. Arlequin (version 3.0): an integrated software package for population genetics data analysis. Evolutionary Bioinformatics Online. 2005; 1:47–50. [PubMed: 19325852]

Frydas, D.; Keupp, H. Berliner geowissenschaftliche Abhandlungen. Vol. E18. Berlin: 1996. Biostratigraphic results in Neogene deposits of NW Crete, Greece, based on calcareous nannofossils; p. 169-189.

Frydas D, Keupp H. The Miocene/Pliocene boundary in NW Crete by means of calcareous nannofossil assemblages. Berliner geowissenschaftliche Abhandlungen. 2001; E36:27–33.

Gantenbein B, Keightley PD. Rates of molecular evolution in nuclear genes of East Mediterranean scorpions. Evolution. 2004; 58:2486–2497. [PubMed: 15612292]

Garcia-Castellanos D, Estrada F, Jiménez-Munt I, Gorini C, Fernández M, Vergés J, De Vicente R. Catastrophic flood of the Mediterranean after the Messinian salinity crisis. Nature. 2009; 462:778–782. [PubMed: 20010684]

Hardie LA, Lowenstein TK. Did the Mediterranean Sea dry out during the Miocene? A reassessment of the evaporite evidence from DSDP legs 13 and 42A cores. Journal of Sedimentary Research. 2004; 74:453–461.

Hay WW, Soeding E, DeConto RM, Wold CN. The Late Cenozoic uplift – climate change paradox. International Journal of Earth Sciences (Geologische Rundschau). 2002; 91:746–774.

Head MJ, Gibbard PL. Early–Middle Pleistocene transitions: the land and ocean evidence. Geological Society, London, Special Publications. 2005; 247:1–18.

Hsü KJ, Montadert L, Bernoulli D, Cita MB, Erickson A, Garrison RE, Kidd RB, Mèlierés F, Müller C, Wright R. History of the Mediterranean salinity crisis. Nature. 1973; 267:399–403.

Huelsenbeck JP, Rannala B. Frequentist properties of Bayesian posterior probabilities of phylogenetic trees under simple and complex substitution models. Systematic Biology. 2004; 53:904–913. [PubMed: 15764559]

Huelsenbeck, JP.; Ronquist, F. Bayesian analysis of molecular evolution using MrBayes. In: Nielsen, R., editor. Statistical methods in molecular evolution. New York: Springer; 2005. p. 183-232.

Jaffey N, Robertson A. Non-marine sedimentation associated with Oligocene–Recent exhumation and uplift of the Central Taurus Mountains, S Turkey. Sedimentary Geology. 2005; 173:53–89.

James GA, Wynd JG. Stratigraphic nomenclature of Iranian Oil Consortium Agreement Area. American Association of Petroleum Geologists Bulletin. 1965; 49:2182–2245.

Jdeidi, T. PhD Thesis. Ankara, Turkey: Middle East Technical University; 2000. Enzyme polymorphism, morphometric and bioacoustic studies in water frog complex in Turkey.

Kasapidis P, Magoulas A, Mylonas M, Zouros E. The phylogeography of the gecko *Cyrtopodion kotschyi* (Reptilia: Gekkonidae) in the Aegean archipelago. Molecular Phylogenetics and Evolution. 2005; 35:612–623. [PubMed: 15878130]

Kass RE, Raftery AE. Bayes factors. Journal of the American Statistical Association. 1995; 90:773–795.

Kosswig C. Zoogeography of the Near East. Systematic Zoology. 1955; 4:49–73.

Krijgsman W, Hilgen FJ, Raffi I, Sierro FJ, Wilson DS. Chronology, causes and progression of the Messinian salinity crisis. Nature. 1999a; 400:652–655.

Krijgsman W, Langereis CG, Zachariasse WJ, Boccaletti M, Moratti G, Gelati R, Iaccarino S, Papani G, Villa G. Late Neogene evolution of the Taza-Guercif Basin (Rifian Corridor, Morocco) and implications for the Messinian Salinity Crisis. Marine Geology. 1999b; 153:147–160.

Kukla, GJ. Loess stratigraphy of Central Europe. In: Butzer, KW.; Isaac, GL., editors. After the Australopithecines: stratigraphy, ecology and culture change in the Middle Pleistocene. Mouton: The Hague; 1975. p. 99-188.

Kukla GJ. Pleistocene land–sea correlations. I. Europe. Earth Sciences Reviews. 1977; 13:307–374.

Kukla GJ. The classical European glacial stages: correlation with deep-sea sediments. Transactions of the Nebraska Academy of Science. 1978; 6:57–93.

Loget N, van den, Driessche J, Davy P. How did the Messinian Salinity Crisis end? Terra Nova, 17. 2005:414–419.

Lymberakis P, Poulokakis N, Manthalou G, Tsigenopoulos CS, Magoulas A, Mylonas M. Mitochondrial phylogeography of *Rana* (*Pelophylax*) populations in the Eastern Mediterranean region. Molecular Phylogenetics and Evolution. 2007; 44:115–125. [PubMed: 17467301]

Maca-Meyer N, Carranza S, Rando JC, Arnold EN, Cabrera VM. Status and relationships of the extinct giant Canary Island lizard *Gallotia goliath* (Reptilia: Lacertidae), assessed using ancient mtDNA from its mummified remains. Biological Journal of the Linnean Society. 2003; 80:659–670.

Meijer PT, Krijgsman W. A quantitative analysis of the desiccation and re-filling of the Mediterranean during the Messinian Salinity Crisis. Earth and Planetary Science Letters. 2005; 240:510–520.

Médail F, Diadema K. Glacial refugia influence plant diversity patterns in the Mediterranean Basin. Journal of Biogeography. 2009; 36:1333–1345.

Meyer, A. Evolution of mitochondrial DNA in fishes. In: Hochachka, PW.; Mommsen, TP., editors. Molecular biology frontiers, biochemistry and molecular biology of fishes. Vol. Vol. 2. New York: Elsevier Science Publisher; 1993. p. 1-38.

Molnar P, England P. Late Cenozoic uplift of mountain ranges and global climate change: chicken or egg? Nature. 1990; 346:29–34.

Mudelsee M, Schulz M. The Mid-Pleistocene climate transition: onset of 100 ka cycle lags ice volume build-up by 280 ka. Earth and Planetary Science Letters. 1997; 151:117–123.

Nei, M. Molecular evolutionary genetics. New York: Columbia University Press; 1987.

Orszag-Sperber F. Changing perspectives in the concept of “Lago-Mare” in Mediterranean Late Miocene evolution. Sedimentary Geology. 2006; 188–189:259–277.

Parmakelis A, Pfenninger M, Spanos L, Papagiannakis G, Louis C, Mylonas M. Inference of a radiation in *Mastus* (Gastropoda, Pulmonata, Enodae) on the island of Crete. Evolution. 2005; 59:991–1005. [PubMed: 16136799]

Parmakelis A, Stathi I, Chatzaki M, Simaiakis S, Spanos L, Louis C, Mylonas M. Evolution of *Mesobuthus gibbosus* (Brullé, 1832) (Scorpiones: Buthidae) in the northeastern Mediterranean region. Molecular Ecology. 2006; 15:2883–2894. [PubMed: 16911208]

Paulo OS, Pinheiro J, Miraldo A, Bruford MW, Jordan WC, Nichols RA. The role of vicariance vs. dispersal in shaping genetic patterns in ocellated lizards in the western Mediterranean. Molecular Ecology. 2008; 17:1535–1551.

Plötner, J. Die westpaläarktischen Wasserfrösche. Von Märtyrern der Wissenschaft zur biologischen Sensation. Laurenti, Bielefeld: Zeitschrift für Feldherpetologie, Beiheft 9; 2005.

Plötner J, Ohst T. New hypothesis on the systematics of the western Palearctic water frog complex (Anura: Ranidae). Mitteilungen aus dem Museum für Naturkunde in Berlin, Zoologische Reihe. 2001; 77:5–21.

Plötner J, Ohst T, Böhme W, Schreiber R. Divergence in mitochondrial DNA of Near Eastern water frogs with special reference to the systematic status of Cypriote and Anatolian populations (Anura, Ranidae). Amphibia-Reptilia. 2001; 22:397–412.

Plötner, J.; Köhler, F.; Uzzell, T.; Beerli, P. Molecular systematics of amphibians. In: Heatwole, H., editor. Amphibian biology, Vol. 7: Phylogeny and systematics. Chipping Norton, Australia: Surrey Beatty & Sons; 2007. p. 2672-2756.

Plötner J, Uzzell T, Beerli P, Spolsky C, Ohst T, Litvinchuk SN, Guex G-D, Reyer H-U, Hotz H. Widespread unidirectional transfer of mitochondrial DNA: a case in western Palearctic water frogs. Journal of Evolutionary Biology. 2008; 21:668–681. [PubMed: 18373588]

Plötner J, Köhler F, Uzzell T, Beerli P, Schreiber R, Guex G-D, Hotz H. Evolution of serum albumin intron-1 is shaped by a 5’ truncated non-long terminal repeat retrotransposon in western Palearctic water frogs (Neobatrachia). Molecular Phylogenetics and Evolution. 2009; 53:784–791. [PubMed: 19665056]

Plötner, J.; Uzzell, T.; Beerli, P.; Akın, Ç.; Bilgin, CC.; Haefeli, C.; Ohst, T.; Köhler, F.; Schreiber, R.; Guex, G-D.; Litvinchuk, AN.; Westaway, R.; Reyer, H-U.; Hotz, H. Genetic divergence and evolution of reproductive isolation in eastern Mediterranean water frogs. In: Glaubrecht, M.; Schneider, H., editors. Evolution in action. Case studies in adaptive radiation and the origin of biodiversity. Special volume from the SPP 1127 “Radiations – Genesis of Biological diversity” of the DFG. Heidelberg, Berlin: Springer; in press

Ponikarov, VP.; Kazmin, VG.; Mikhailov, IA.; Razvaliayev, AV.; Krasheninnikov, VA.; Kozlov, VV.; Soulidi-Kondratiyev, ED.; Mikhailov, KY.; Kulakov, VV.; Faradzhev, VA.; Mirzayev, KM. Explanatory notes on the geological map of Syria, scale 1:500,000. Part I, Stratigraphy, Igneous Rocks and Tectonics. Moscow, Syrian Arab Republic, Damascus: Ministry of Industry; 1967. The geology of Syria. Vsesojuznoje Exportno-Importnoje Objedinenije “Technoexport”

Posada D. ModelTest Server: a web-based tool for the statistical selection of models of nucleotide substitution online. Nucleic Acids Research. 2006; 34:W700–W703. doi:10.1093/nar/gkl042. [PubMed: 16845102]

Posada D, Crandall KA. Modeltest: testing the model of DNA substitution. Bioinformatics. 1998; 14:817–818. [PubMed: 9918953]

Robertson AHF. Late Miocene paleoenvironments and tectonic setting of the southern margin of Cyprus and the Eratosthenes Seamount. Proceedings of the Ocean Drilling Program –Scientific Results. 1998; 160:453–463.

Robertson A, Ünlügenç ÜC, İnan N, Taşlı K. The Misis-Andırın complex: a Mid-Tertiary melange related to late-stage subduction of the Southern Neotethys in S Turkey. Journal of Asian Earth Sciences. 2004; 22:413–453.

Ronquist F, Huelsenbeck JP. MRBAYES 3: Bayesian phylogenetic inference under mixed models. Bioinformatics. 2003; 19:1572–1574. [PubMed: 12912839]

Rouchy JM, Caruso A. The Messinian salinity crisis in the Mediterranean basin: A reassessment of the data and an integrated scenario. Sedimentary Geology. 2006; 188–189:35–67.

Roveri M, Manzi V. The Messinian salinity crisis: Looking for a new paradigm? Palaeogeography, Palaeoclimatology, Palaeoecology. 2006; 238:386–398.

Sampalmieri G, Iadanza A, Cipollati P, Casentino D, Lo Mastro S. Palaeoredox indicators from the organic-rich Messinian early post-evaporitic deposits of the Apennines (Central Italy). Geophysical Research Abstracts. 2009; 11 EGU2009-12716-6.

Schneider H, Sinsch U. Taxonomic reassessment of Middle Eastern water frogs: bioacoustic variation among populations considered as *Rana ridibunda*, *R. bedriagae* or *R. levantina*. Journal of Zoological Systematics and Evolutionary Research. 1999; 37:57–65.

Seyrek A, Demir T, Pringle M, Yurtmen S, Westaway R, Bridgland D, Beck A, Rowbotham G. Late Cenozoic uplift of the Amanos Mountains and incision of the Middle Ceyhan river gorge, southern Turkey; Ar-Ar dating of the Düziçi basalt. Geomorphology. 2008a; 97:321–355.

Seyrek A, Westaway R, Pringle M, Yurtmen S, Demir T, Rowbotham G. Timing of the Quaternary Elazığ volcanism, eastern Turkey, and its significance for constraining landscape evolution and surface uplift. Turkish Journal of Earth Sciences. 2008b; 17:497–541.

Sosdian S, Rosenthal Y. Deep-sea temperature and ice volume changes across the Pliocene-Pleistocene climate transitions. Science. 2009; 325:306–310. [PubMed: 19608915]

Steininger, FF.; Rögl, F. Paleogeography and palinspastic reconstruction of the Neogene of the Mediterranean and Paratethys. In: Dixon, JE.; Robertson, AHF., editors. The geological evolution of the Eastern Mediterranean. Vol. 17. Geological Society, London: Special Publications; 1984. p. 659-668.(reprinted 1996)

Sumida M, Kanamori Y, Kaneda H, Kato Y, Nishioka M, Hasegawa M, Yonekawa H. Complete nucleotid sequence and gene rearrangement of the mitochondrial genome of the Japanese pond frog *Rana nigromaculata*. Genes & Genetic Systems. 2001; 76:311–325. [PubMed: 11817647]

Tamura K, Nei M. Estimation of the number of nucleotide substitutions in the control region of mitochondrial DNA in humans and chimpanzees. Molecular Biology and Evolution. 1993; 10:512–526. [PubMed: 8336541]

Tamura K, Dudley J, Nei M, Kumar S. MEGA4: Molecular Evolutionary Genetics Analysis (MEGA) software version 4.0. Molecular Biology and Evolution. 2007; 24:1596–1599. [PubMed: 17488738]

Templeton AR. Statistical phylogeography: methods of evaluating and minimizing inference errors. Molecular Ecology. 2004; 13:789–809. [PubMed: 15012756]

Welter-Schultes FW, Williams MR. History, island area and habitat availability determine land snail species richness of Aegean islands. Journal of Biogeography. 1999; 26:239–249.

Westaway R, Demir T, Seyrek A. Geometry of the Turkey-Arabia and Africa-Arabia plate boundaries in the latest Miocene to Mid-Pliocene: the role of the Malatya-Ovacık Fault Zone in eastern Turkey. eEarth. 2008; 3:27–35.

Westaway R, Bridgland DR, Sinha R, Demir T. Fluvial sequences as evidence for landscape and climatic evolution in the Late Cenozoic: a synthesis of data from IGCP 518. Global and Planetary Change. 2009a; 68:237–253.

Westaway R, Guillou H, Seyrek A, Demir T, Bridgland D, Scaillet S, Beck A. Late Cenozoic surface uplift, basaltic volcanism, and incision by the River Tigris around Diyarbakır, SE Turkey. International Journal of Earth Sciences. 2009b; 98:601–625.

## Biography

The authors are interested in the phylogeography, genetics, systematics and evolution of Western Palaearctic water frogs, except for R.W., who is an Earth Scientist.

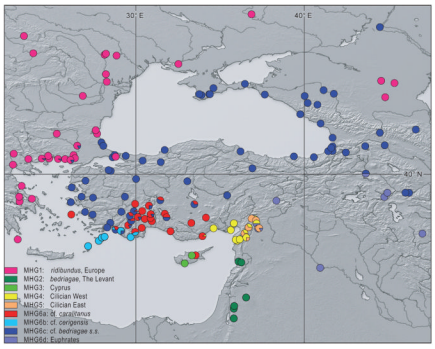


**Figure 1.**
Distribution of the main haplogroups (MHG) and subgroups (a–d) of water frogs (genus *Pelophylax*) in the eastern Mediterranean region.

**Figure 2.**
MrBayes maximum posterior tree of mitochondrial haplotypes determined on the basis of concatenated ND2 and ND3 sequences (1378 bp) obtained from Western Palaearctic water frogs (genus *Pelophylax*) and the Eastern Palaearctic water frog species *P. nigromaculatus*. The values at the branches are posterior probabilities for the clade to the right of that branch. The unit of the scale bar is equivalent to the expected mutations per site. The terminal labels are combinations of the haplotype IDs of the ND2 and ND3 genes (Appendix S2). Sequence numbers are specified in Appendix S2.

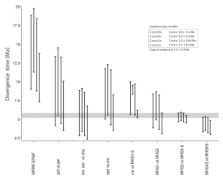

**Figure 3.**

Divergence time (95% credibility intervals) estimated for the following eight comparisons: Western Palaearctic water frogs (WPWF) versus Eastern Palaearctic water frogs (EPWF), *Pelophylax saharicus* (*sah*) vs. *P. perezi* (*per*), *P. lessonae* (*les*) and *P. bergeri* (*ber*) vs. *P. shqipericus* (*shq*), *P. epeiroticus* (*epe*) vs. *P. cretensis* (*cre*), *P. cretensis* (*cre*) vs. MHG1-9, MHG1 (*P. ridibundus* Central Europe) vs. MHG2 (*P. bedriagae*), MHG3 (Cyprus) vs. MHG4-9, MHG4-5 (Cilician groups) vs. MHG6-9. Four scenarios (CRETE9w, CRETE9n, CRETE5w and CRETE5n) are listed from top to bottom in the box and from left to right in each group of comparisons. All four scenarios assume a mean isolation time for Cyprus of 5.3±0.3 Ma; scenario CRETE9 assumes a mean isolation time of 9.0 Ma for Crete, whereas scenario CRETE5 assumes a mean isolation time of 5.3 Ma; n and w in the scenarios names refer to narrow (±0.3 Ma) and wide (0.5 × mean isolation time) standard deviations around the isolation time of Crete. The grey line indicates the period from the start to the end of the MSC. BEAST was performed on the basis of 83 concatenated ND2 and ND3 sequences.

**Table 1**

Estimates of divergence times between several main haplogroups (MHG) and subgroups (6a–6d) of water frogs (genus *Pelophylax*) in the eastern Mediterranean region based on mean Tamura-Nei distances (TrN) with a gamma-distributed shape parameter G=0.2. Divergence times were calculated by dividing two putative evolutionary rates (TrN+$G_{5.3}$=1.7% $Myr^{-1}$; TrN+$G_{5.5}$ =1.6% $Myr^{-1}$) through the divergence values (Regression), and obtained directly on the neighbour-joining tree as implemented in MEGA 4.1. Evolutionary rates were estimated assuming two different divergence times (5.3 and 5.5 million years ago, Ma) between water frog populations of Cyprus (MHG3) and Anatolian populations represented by MHG4,5, and 6. Additionally, divergence times where calculated with BEAST using variable evolutionary rates and 2 calibration points (MHG3-sister clade at 5.3±0.3 Ma and *P. cretensis*-sister clade at 9.0±0.3 Ma) using the tree prior for all values shown, the tree prior was a Yule process. LRCA: last recent common ancestor.

| Comparison | TrN+G | Divergence time estimates (Ma) | | | |
|---|---|---|---|---|---|
| | | Regression model | MEGA | BEAST | |
| | | | | Mean | 95% credibility |
| MHG1-MHG3-9 | 0.098 | 5.76–6.12 | 5.66–5.88 | 6.21 | 5.06–7.50 |
| MHG2-MHG1+3-9 | 0.091 | 5.35–5.69 | 5.35–5.55 | 7.19 | 5.80–8.51 |
| MHG3-MHG4/5 | 0.100 | - | - | 5.38* | 4.82–5.92* |
| MHG4-MHG5 | 0.047 | 2.76–2.94 | 2.75–2.85 | 3.04 | 1.58–4.38 |
| MHG4/5-MHG6 | 0.050 | 2.94–3.12 | - | 4.47 | 3.49–5.34 |
| MHG4/5-MHG6-9 | 0.052 | 3.06–3.25 | 3.11–3.15 | 4.47 | 3.49–5.34 |
| MHG6a–MHG6b | 0.026 | 1.53–1.62 | - | 3.07 | 2.07–4.07 |
| MHG6a–MHG6c | 0.019 | 1.12–1.19 | - | - | - |
| MHG6a–MHG6d | 0.024 | 1.41–1.50 | - | - | - |
| MHG6b–MHG6c | 0.019 | 1.12–1.19 | - | - | - |
| MHG6b–MHG6d | 0.025 | 1.47–1.56 | - | - | - |
| MHG6c–MHG6d | 0.018 | 1.06–1.12 | - | - | - |
| LRCA of MHG6 | - | - | 1.19–1.24 | - | - |
| MHG6-MHG7 | 0.035 | 2.06–2.19 | 2.05–2.12 | - | - |
| MHG8-MHG9 | 0.032 | 1.88–2.00 | 1.91–1.98 | 2.17 | 0.78–3.62 |
| MHG6/7-MHG8/9 | 0.053 | 3.12–3.31 | 3.11–3.22 | 4.23 | 3.19–5.16 |
| *P. cretensis*-MHG1-9 | 0.228 | 13.41–14.25 | 13.40–13.91 | 8.93* | 8.34–9.50* |

*Calibrated with a strong prior distribution